
Article:
Petridi, Stavroula, Middleton, C. Adam, Ugbode, Christopher orcid.org/0000-0002-6023-8294 et al. (3 more authors) (2020) In vivo visual screen for dopaminergic Rab ⇿ LRRK2-G2019S interactions in Drosophila discriminates Rab10 from Rab3. G3: Genes, Genomes, Genetics. ISSN 2160-1836

In vivo visual screen for dopaminergic *Rab* ↭ *LRRK2-G2019S* interactions in *Drosophila* discriminates *Rab10* from *Rab3*

Stavroula Petridi[1,2], C. Adam Middleton[1], Chris Ugbode[1], Alison Fellgett[1], Laura Covill[1,3] & Christopher J. H. Elliott[1]

1) Department of Biology and York Biomedical Research Institute, University of York, York, YO1 5DD, UK

Present addresses:
2) School of Life Sciences, University of Warwick, Gibbet Hill Campus, Coventry CV4 7AL, UK
3) Department of Haematology and Regenerative Medicine, Karolinska Institutet, Blickavägen 8, Huddinge, Stockholm, Sweden.

Running title: Dopaminergic Rab ⇿ LRRK2-G2019S interactions

Correspondence to CJHE – Department of Biology, University of York, York, YO10 5DD, UK.

Email: cje2@york.ac.uk
Tel: +44 1904 328654

Keywords: *LRRK2, G2019S, Rab10, Rab3, Drosophila melanogaster, Parkinson's disease*

Author contributions: SP, CAM, CU, AF, LC and CJHE performed experiments, CJHE drafted the manuscript, and SP, CAM, CU, AF, LC and CJHE revised the manuscript.

No conflicts of interest were perceived.

Abstract

LRRK2 mutations cause Parkinson's, but the molecular link from increased kinase activity to pathological neurodegeneration remains undetermined. Previous *in vitro* assays indicate that LRRK2 substrates include at least 8 Rab GTPases. We have now examined this hypothesis *in vivo* in a functional, electroretinogram screen, expressing each *Rab* with/without *LRRK2-G2019S* in selected *Drosophila* dopaminergic neurons. Our screen discriminated Rab10 from Rab3. The strongest Rab/LRRK2-G2019S interaction is with Rab10; the weakest with Rab3. Rab10 is expressed in a different set of dopaminergic neurons from Rab3. Thus, anatomical and physiological patterns of Rab10 are related. We conclude that Rab10 is a valid substrate of LRRK2 in dopaminergic neurons *in vivo*. We propose that variations in *Rab* expression contribute to differences in the rate of neurodegeneration recorded in different dopaminergic nuclei in Parkinson's.

Introduction

Inherited mutations in *LRRK2* (*Leucine-rich-repeat kinase 2*) are a common cause of Parkinson's. A single amino-acid change, *G2019S*, increases LRRK2 kinase activity (Greggio and Cookson 2009). This mutation results in a toxic cascade that kills *substantia nigra* dopaminergic neurons. However, the main steps in this pathological signalling pathway remain to be determined. Partly this is because LRRK2 is potentially a multi-functional protein, with kinase, GTPase and protein-binding domains. A diverse range of >30 proteins that might be phosphorylated by LRRK2 have been reported, suggesting it is a generalised kinase (Tomkins *et al.* 2018). However, several research teams have recently reported that LRRK2 is a more specific kinase, phosphorylating a range of Rab GTPases (Thirstrup *et al.* 2017; Steger *et al.* 2017; Fan *et al.* 2018; Liu *et al.* 2018; Jeong *et al.* 2018; Kelly *et al.* 2018).

Rabs are a plausible LRRK2 substrate leading to neurodegeneration, as they act as molecular switches interacting with a range of proteins (GEFs, GAPs and GDIs) regulating supply and delivery of cargo to membranes. Indeed many of the 66 Rabs in humans have been linked to neurodegenerative disorders (Kiral *et al.* 2018). Mutations in Rabs 29 and 39 cause Parkinson's (MacLeod *et al.* 2013; Beilina *et al.* 2014; Wilson *et al.* 2014). Biochemically, at least 8 seem to be directly phosphorylated by LRRK2 [Rabs 3, 5, 8, 10, 12, 29, 35 and 43] (Steger *et al.* 2017). However, it is not clear which of the more than 60 Rabs are actually phosphorylated *in vivo*. In mammals, analysis of the role of the Rabs is complex because individual Rabs may have similar, or even compensatory functions, which may differ by tissue (Chen *et al.* 2012; Kelly *et al.* 2018). The situation is simpler in the fly, because there are fewer Rabs - only 23 mammalian orthologs. Here, we use a *Drosophila* screen to assess the link from LRRK2 to Rabs *in vivo* using the *Tyrosine Hydroxylase* (*TH*) GAL4 to achieve dopamine specific expression. UAS-*LRRK2-G2019S* (Liu *et al.* 2008) was driven with and without each *Rab* gene (Zhang *et al.* 2006).

We measured a visual phenotype using the SSVEP (Steady State Visual Evoked Potential). Although the outer structure of the eye differs markedly between flies and mammals, the retinal circuitry is highly similar (Cajal and Sanchez 1915; Sanes and Zipursky 2010) – importantly both contain dopaminergic neurons. In the human, the retinal dopaminergic neurons die in Parkinson's (Harnois and Di Paolo 1990), while in the *TH>G2019S* model of Parkinson's, the retina has visual deficits, including neurodegeneration (Hindle *et al.* 2013; Afsari *et al.* 2014; West *et al.* 2015a). We can now use the ability of the SSVEP assay to separate and quantify the response of the photoreceptors and lamina neurons to go beyond measuring neurodegeneration, but to test for a synergistic interaction of a Parkinson's related gene with potential substrates. Notably, we can do this *in vivo* in young flies before degeneration has set in.

We determined that, *in vivo*, Rab10 has the strongest synergy with LRRK2-G2019S, Rab3 the weakest. We validated the physiological results by showing differences in the expression of *Rab10* and *Rab3* in visual dopaminergic interneurons.

Materials and methods

Flies (*Drosophila melanogaster*) were raised and manipulated according to standard fly techniques. Fly stocks are listed in Table 1. Crosses were raised at 25 °C on a 12:12 light-dark cycle. On the day of emergence, female flies were placed in the dark at 29 °C.

Screen design: Virgins from the *TH*-GAL4, or from a *TH*-GAL4::UAS-*LRRK2-G2019S* (*THG2*) recombinant were crossed with males carrying UAS-*Rab*, for each of the *Rabs* that are homologous to those of mammals.

The principle of the SSVEP screen is shown in Fig. 1. The visual response of flies stimulated with a flickering blue light was recorded. Young, 4-12 hour old, PD-mimic flies show visual hyperexcitability, particularly in the lamina

neurons (Afsari *et al.* 2014; Himmelberg *et al.* 2017). This includes the *THG2* flies. As they age, the visual response gets weaker and vanishes by 28 days. We therefore chose to test flies aged for 24-36 hours (1 day) or 1 week - between the time at which *G2019S* expression results in hyperexcitability and the time at which degeneration is first noted. At these time points, the mean visual response of dark-reared *THG2* flies was similar to the *TH/+* controls.

Sample test for synergy: We test for an interaction between *Rab7* and *G2019S* in dopaminergic neurons as follows: we compare flies expressing both *Rab7* and *G2019S* transgenes (*THG2* > *Rab7*) with flies expressing just one transgene (*TH* > *Rab7* or *THG2*) and control flies with no transgene expression (*TH/+*) (Fig. 1F). The average visual response of *TH* > *Rab7* and *THG2* flies is very similar to the control flies – there is no mean difference for either the photoreceptors or lamina neurons. We do note that the *THG2* flies have a larger variability than the *TH/+* flies, particularly in the lamina neurons (Fig. 1F). However, in flies with dopaminergic expression of both *G2019S* and *Rab7*, the photoreceptor and lamina neuron responses were much increased (4.1x and 8.8x, both $P < 0.001$). This demonstrates that dopaminergic neurons with both *Rab7* and *G2019S* have a synergistic hyperexcitable visual phenotype.

SSVEP preparation: At the required age, flies were prepared for SSVEP measurements using a pooter and nail polish to secure them in the cut-off tip of a pipette tip, without anaesthesia (Fig. 1B). Each fly was presented 5 times with a set of 9 flickering stimuli. In each stimulus, the average light intensity was the same, but the amplitude of the flicker was adjusted from 10 to 100%, giving a range of contrasts. Sample stimuli are shown in Fig. 1C. Offline, the Fast-Fourier Transform was applied to the responses, to separate the first harmonic (1F1), due to the photoreceptors from the second harmonic (2F1), due to the lamina neurons (Fig. 1D). Other harmonics present in the data were not analysed. For these first two harmonics, we plotted the contrast response function for each fly (Fig. 1E) and determined the best response of

that fly. This allowed us to determine the average visual performance for each cross (Fig. 1F). This data pipeline is the same as that devised by Afsari *et al.* (2014), but using an Arduino Due to generate the stimuli and record the responses instead of a PC. Data were analysed in Matlab, Excel and R. Full code at https://github.com/wadelab/flyCode.

Immunocytochemistry was performed as described recently (Cording *et al.* 2017). Tyrosine hydroxylase was detected with Mouse anti TH Immunostar (22941, 1:1000). Fluorescent reporters (nRFP, eIf-GFP) were expressed in dopaminergic neurons using the *TH*-GAL4. Images were prepared for publication using ImageJ; original images are available on request.

Western blots for EYFP, encoded in each Rab transgene were made from non-boiled fly head lysates, run on Novex pre-cast mini gels (NuPAGE 4-12% Bis-Tris Gels, NP0322BOX, Thermo Scientific) in 1 x MOPS buffer and transferred onto PVDF membranes using a Hoefer wet transfer tank (TE22) at 100V for 1 hr. Membranes were probed with Guinea pig anti-GFP (Synaptic Systems, 1:1000). For detection of LRRK2 protein, boiled lysates were run on 4-20% Mini-PROTEAN TGX Precast gradient gels and transferred using the same method. Membranes were probed with anti-LRRK2 (Neuromab, clone N241A/34, 1:1000). α-drosophila synaptotagmin was used as a loading control (West *et al.* 2015b). Densitometric analysis was carried out using ImageJ.

Statistics were calculated in R, with the mean ± SE reported by error bars or median ± interquartile range in box plots. Post-hoc tests were calculated for ANOVA using the Dunnett test.

Data Availability Statement: Data tables (Excel sheets) and R code are open access on GitHub: https://github.com/wadelab/flyCode/tree/master/analyzeData/fly_arduino/G3 . Raw images and SSVEP traces are available on request. No new reagents are described.

Results

A visual expression screen identifies that Rab10 has the strongest genetic interaction with LRRK2-G2019S; Rab3 the weakest

In order to identify the Rabs which show a strong synergy with *LRRK2-G2019S* we compared the increase in visual response due to expression of the *Rab* by itself (X in Fig. 1F, X-axis in Fig. 2A) against the further increase in visual response when both *Rab* and *G2019S* are expressed (Y in Fig. 1F, Y-axis in Fig. 2A). This plot places the Rabs along a spectrum, from those that interact synergistically with *G2019S* (top left) to those with a little or no interaction (bottom right). Thus, for some Rabs (10, 14, 27, 26) expression of both *G2019S* and the *Rab* in dopaminergic neurons leads to a big increase in the lamina neuron response. Interestingly, these Rabs have little effect when expressed alone. The converse is also true: for the *Rabs* with the biggest effect (3, 32, 1), adding *G2019S* has no further effect. This is true for both components of the SSVEP signal – that from the lamina neurons is higher, but parallel to the photoreceptor signal.

We wanted to examine which factors controlled this synergy. A number of hypotheses have been put forward in the LRRK2/Rab literature. First, Rabs previously linked to Parkinson's (Shi *et al.* 2017), either through population studies or through potential actions with Parkinson's-related genes, generally have a stronger response to *G2019S* than others (Fig. 2Bi). Indeed, the Rab furthest above the regression line is one that causes Parkinson's, *Rab39* (Wilson *et al.* 2014). Next, we tested if Rabs with a high degree of phylogenetic similarity clustered systematically, but did not find any difference (Fig. 2Bii). Then we examined where, on our spectrum, the Rabs phosphorylated *in vitro* [3, 5, 8, 10, 12, 29, 35 and 43] might lie. There is no close homolog for Rabs 12, 29 or 43. Rabs 3, 5 and 8 are on the right of the spectrum, Rab35 in the middle and Rab10 on the top-left, so no clear pattern emerges. The *in vitro* data suggest that LRRK2-G2019S preferentially phosphorylates Rabs with Thr rather than Ser at the active site (Steger *et al.* 2016), but this is not evident from

the spectrum. Neither *in vitro* evidence for phosphorylation of the Rab by LRRK2, nor the amino-acid at the active site affects the regression (Fig. 2Biii,iv). We also noted that, in cell based assays, LRRK/Rab interactions have been noted at mitochondria (Wauters *et al.* 2019), lysosomes (Eguchi *et al.* 2018) or Golgi (Liu *et al.* 2018). Thus, we tested if the 'main' organelle associated with the Rab (Banworth and Li 2017) affected the position of a Rab on the spectrum, but found no sign that this affected the regression (Fig. 2Bv). However, the Rabs placed in the middle of the spectrum [2, 6, 9, 18] are linked to traffic in the Golgi or ER-Golgi.

Thus, the relationship between visual impact of *Rab* and impact of *Rab* + *G2019S* identifies 10, 14, 27 as having the strongest synergy. This holds for the responses of both photoreceptors and lamina neurons, with the same Rabs found clustered at each end of the spectrum.

The Rab10/G2019S *interaction enhances neuronal signalling*

Normally, flies with more excitable photoreceptors activate the lamina neurons more strongly, though there is some adaptation. The SSVEP response can be decomposed into two components – 1F1 and 2F1, corresponding to activity in the photoreceptors and lamina neurons respectively. This allows us to test the physiological relationship between the photoreceptors and lamina neurons, and to see if any Rab disrupts the retinal neuronal circuitry. Generally, as the photoreceptor response increases, so does the lamina neuron response (Fig. 3). This relationship is remarkably similar in young (day 1) and older (day 7) flies. However, there is a one marked outlier, *Rab10*, where the lamina neuron response at day 1 is ~5 times the value expected from the regression, and at day 7 is substantially below the line. Thus, in young *THG2* > *Rab10* flies there is much greater neuronal activity than expected, but in 1-week old *THG2* > *Rab10* flies we observe reduced activity, suggesting neurodegeneration has begun. Young and old Rab3 flies lie on the regression, close to the origin, very different from Rab10.

Thus our screen highlights a major difference between two of the Rabs that are phosphorylated in vitro: *Rab3* expression in dopaminergic neurons has a big increase in visual sensitivity, but no further effect when *G2019S* is added, whereas Rab10 expression has little effect by itself, but a massive effect in young flies with *G2019S.*

Why might G2019S interact so strongly with Rab10 but have no effect on Rab3?

As LRRK2 is a human protein, and the Rabs we expressed were native *Drosophila* proteins, one possibility is that the fly and human Rabs are sufficiently different that LRRK2-G2019S can phosphorylate fly Rab10 but not fly Rab3. This seems very unlikely as the hRab3 / dRab3 and dRab10 / hRab10 sequences are very similar, indeed they are identical over the GTP binding domain and LRRK2 phosphorylation sites (Fig. 4). A second explanation for the difference between Rab10 and Rab3 is that the *Rab* and/or *G2019S* is not expressed to the same extent. Western Blots of *THG2* > *Rabs 3, 39* or *10* were probed for LRRK2, and compared with *THG2*. Essentially the same level of protein was measured (Fig. 5A). This is not unexpected, as each cross contains the same GAL4 and UAS-*LRRK2-G2019S* constructs. A second set of blots were probed for EYFP, as each of the UAS-*Rab* lines carries an EYFP fusion. This showed that the levels of Rab10 and Rab39 were similar, though Rab3 was less at about 50% (Fig. 5B). The reduced level of Rab3 may arise from the different insertion site, or from a more rapid breakdown during synaptic signalling. The differences in level of Rab proteins are not sufficient to explain the physiological differences.

We therefore wondered if the stronger synergy between G2019S and Rab10, compared with Rab3, might result from a difference in the anatomical distribution of the Rabs (along with their GEFS, GAPs and effectors) among fly dopaminergic neurons.

Rab10 and Rab3 are found in different dopaminergic neurons

The fly visual system is innervated by three kinds of dopaminergic neurons (Hindle *et al.* 2013), the MC neurons in the medulla, and two type of PPL neurons, which innervate either lobula or lamina respectively. These, and the other clusters of dopaminergic neurons, are reliably marked by α-TH antibody, which binds in the cytoplasm.

To examine the overall distribution of Rab10, we used *Rab10*-GAL4 (Chan *et al.* 2011) to express either a RFP which strongly localises to the nucleus, or a GFP with mainly nuclear localisation. These fluorescent constructs have two advantages: (i) they provide a reduced background compared with membrane localised reporters, and (ii) the nuclear fluorescence is contained within the cytoplasmic signal from α-TH, reducing the problems of determining co-localisation.

Only a small proportion of CNS neurons are Rab10 positive (Fig. 6). We find that some (by no means all) dopaminergic neurons are Rab10 positive (Fig. 6A,B). Even within a cluster, we only detect Rab10 in some neurons; in other neurons in the same cluster Rab10 is undetectable (e.g. PAL, PPL2ab, PPM3 and PAM). The individually identifiable neurons (TH-VUM, TH_AUM, the DADN pair, and T1 pair) were consistently clearly marked. However, in two clusters we saw no evidence for *Rab10* driven fluorescence (PPL2c and PPM1/2).

When we used *Rab3*-GAL4 to drive the same RFP/GFP almost all the neurons were marked (Fig. 6 C, Di). This includes the majority of the dopaminergic neurons, including all the PPL1 (Fig. 6 Dii-iv) and PPL2 neurons.

The MC neurons in the optic lobes were not marked in either the Rab10 or Rab3 experiments (Fig. 6 Aiv, Biv), though other Rab10 / Rab3 positive neurons are present nearby. Since the MC neurons do not generally stain well with GFP (Nassel and Elekes 1992; Hindle *et al.* 2013)), we tested if the MC neurons were detected with *TH*-GAL4 > *nRFP*. This marked all the neurons highlighted by α-TH, except the MC neurons. The MC neurons do express

TH, along with other genes linked to dopamine - *ddc* (*dopa decarboxylase*), *Vmat* (*vesicular monoamine transporter*) and *DAT* (*dopamine transporter*) (Davis *et al.* 2020) so are genuinely dopaminergic. The MC neurons are one of three kinds of Medulla intrinsic neurons that express *Rab10* at high levels, while all the optic lobe neurons (including MC) have high expression of Rab3 (Davis et al, 2020, extended data at http://www.opticlobe.com/).

Thus, we conclude that some of the dopaminergic neurons in the visual system are Rab10 positive. These are some of the PPL cluster that innervate the lobula or project to the lamina, and the MC neurons in the medulla. All dopaminergic neurons are Rab3 positive.

Differences in the loss of dopaminergic neurons between neuronal clusters

Drosophila models of Parkinson's have consistently shown loss of dopaminergic neurons with age when *LRRK2*, α-*synuclein* or *parkin* were manipulated. For *LRRK2*, most of the published information is for the Parkinson's-causative mutations *G2019S* or *I2020T,* driven by *DDC*-GAL4. This expresses in the dopaminergic and some serotonergic neurons. By 6-7 weeks (about two-thirds of the fly lifespan), about 25-50% of the dopaminergic neurons have been lost. For each cluster, there is quite a spread of the data (Fig. 7), which is most likely due to differences in the food used to feed the flies or the genetic background (Lavoy *et al.* 2018; Chittoor-Vinod *et al.* 2020). However, overall, the PAL cluster is much less susceptible to cell loss than the PPL1, PPL2, PPM1/2 or PPM3 clusters.

Discussion

Rab10 shows a strong synergy with LRRK2-G2019S.

The key observation from the screen was that two of the Rabs suggested to be substrates of LRRK2 *in vitro* behave quite differently *in vivo*, in a physiological response to expression in dopaminergic neurons. Rab10 shows a strong

synergy with *G2019S*; Rab3 none. The existence of (*Drosophila*) Rab10 in the tyrosine hydroxylase positive neurons controlling vision (MC and PPL2ab neurons) argues that LRRK2 might indeed phosphorylate dRab10 directly. Thus our *in vivo* results both support the *in vitro* (biochemical and cell culture) data in which LRRK2 directly phosphorylates hRab10 (Thirstrup *et al.* 2017; Steger *et al.* 2017; Fan *et al.* 2018; Liu *et al.* 2018; Jeong *et al.* 2018; Kelly *et al.* 2018). It also implies that the MC / PPL2ab cells contain Rab10 effectors which interact with phospho-dRab10. The results of this will include changes to the cellular homeostasis and physiological responsiveness of dopaminergic neurons. One possible physiological outcome is that Rab10 phosphorylation reduces retinal dopamine release onto the photoreceptors. This will increase the amplitude and speed of the photoreceptor response (Chyb *et al.* 1999). Dopamine may also affect the lamina neurons, and third order MC cells, but it remains to be determined if they have dopamine receptors. It is also possible that p-Rab10 modulates the release of co-transmitters or growth factors from dopaminergic neurons.

A unique feature of the screen is that when *G2019S* and *Rab10* are expressed together the lamina neuron response is much bigger than that predicted from the photoreceptor response. This might arise from the unusual double role of Rab10 – in both exo- and in endo-cytosis (Larance *et al.* 2005; Glodowski *et al.* 2007; Chua and Tang 2018). The best defined role of Rab10 in exocytosis is in adipocytes, as part of the insulin-stimulated release of GLUT4 vesicles, linked to AS/160 (see for review (Jaldin-Fincati *et al.* 2017)). In endocytosis, the effects of Rab10 are mediated through a different pathway, including the EHBP1-EHD2 complex. In the follicle cells of *Drosophila*, *ehbp1* expression and knockdown phenocopy Rab10 manipulations (Isabella and Horne-Badovinac 2016), while EHBP1 was also identified by a systematic proteomic analysis as indirectly phosphorylated by LRRK2 in HEK293 cells (Steger *et al.* 2017) and a lysosomal assay (Eguchi *et al.* 2018). The phosphorylation of Rab10 by LRRK2 may switch its effector, and so activate a different pathway.

A spectrum of Rab ↔ G2019S interactions in vision

Our screen placed the Rabs along a spectrum, ranging from those with a strong synergy with *G2019S* to those which had a strong effect when expressed by themselves.

Among the Rabs which show little synergy with *G2019S* but have strong visual effect are 1, 3, 5, 6 and 11. Two of these Rabs [3,5] are phosphorylated by LRRK2 *in vitro* (Steger *et al.* 2017), but neither synergise with LRRK2-G2019S in the visual assay. Our data suggest Rab3 is not a major substrate of *LRRK2-G2019S* in these dopaminergic neurons, possibly because Rab3 is located synaptically. This may be far from LRRK2 at the trans-Golgi network (Liu *et al.* 2018). The difference between Rab3 and 10 (at opposite ends of our spectrum) is notable because *in vitro* mammalian cell assays have highlighted similar roles of Rabs 3 and 10 in lysosome exocytosis, (Encarnação *et al.* 2016; Vieira 2018).

Rabs 10, 14 and 27 have the strongest synergy with *G2019S*, though by themselves they have little effect on visual sensitivity. Like Rab10, Rabs 14 and 27 have defined roles in exocytosis (Larance *et al.* 2005; Ostrowski *et al.* 2010).

Some Rabs are in the middle of the spectrum [2, 6, 9, 18], with a 2-3 fold increase in visual response when the *Rab* is expressed alone, and a further 2-3 fold increase when both *Rab* and *G2019S* are expressed. These Rabs have been linked to the Golgi, or to Golgi-ER traffic (Banworth and Li 2017). Thus a cellular phenotype parallels the physiological response.

Our observation that every Rab seems to have some effect on dopaminergic signalling in the visual system goes some way to explain why many studies of individual Rabs have demonstrated effects with LRRK2 ; Rab3a (Islam *et al.* 2016); Rab5 (Shin *et al.* 2008); Rab7 (Dodson *et al.* 2012); Rab29 (Beilina *et al.* 2014). Although cellular studies support binding of Rab29 to LRRK2 (Purlyte

et al. 2018), the closest fly homolog (Rab32) shows little synergy with *G2019S* in our screen.

The availability of Rab transgenic flies facilitates screening in *Drosophila*. Screens have identified key roles for Rab2 in muscle T-tubule development (Fujita *et al.* 2017); Rabs 2, 7, 19 in loss of huntingtin (White *et al.* 2015), 1, 5, 7, 11 and 35 in the *Drosophila* renal system (Fu *et al.* 2017), Rab32 in lipid storage (Wang *et al.* 2012) and Rab39 in tracheal formation (Caviglia *et al.* 2016). The varied outcomes of these screens indicate the validity of the LRRK2-G2019S ⇿ Rab10 relationship reported here.

Each dopaminergic neuron has its own palette of Rab expression

Finally, we note that not all dopaminergic neurons are equally susceptible in Parkinson's. A long-standing observation is that the dopaminergic neurons in the VTA (ventral tegmental area) do not degenerate in the same way as those in the *substantia nigra*. More particularly, even within the *substantia nigra* there is a range of outcomes, with dopaminergic neurons in the *pars compacta* dying more than those in the dorsal and lateral zones (Damier *et al.* 1999). The same is true for the fly brain: the neurons in the PPM clusters degenerate more than the PAL (though no data are available for the visual MC neurons). If anything, our data suggest the clusters with less Rab10 have more neurodegeneration. Previously, faster neurodegeneration has been ascribed to increased cytosolic dopamine levels (Burbulla *et al.* 2017), to intracellular effects of glutamate (Steinkellner *et al.* 2018), to increased calcium influx (Guzman *et al.* 2010), to more action potentials (Subramaniam *et al.* 2014), or to longer axons with more synapses (Pacelli *et al.* 2015). It has not escaped our notice that faster degeneration in some neurons may be the result of their different palettes of Rab proteins and their effectors.

401 Figure Legends
402
403
404 Fig. 1. **SSVEP (Steady State Visual Evoked Potential Analysis) measures the**
405 **contrast response function of the insect eye**. A. The fly eye consists of ~800
406 ommatidia, each containing 8 photoreceptors. Their axons project to the
407 lamina and medulla, where they synapse with the second- and third order
408 neurons (lamina and medulla neurons). The medulla contains intrinsic
409 dopaminergic neurons (MC, also called Mi15 neurons (Davis *et al.* 2020)),
410 while some dopaminergic neurons from the CNS project to the lamina. B.
411 Recording the fly visual response: A fly, restrained in a pipette tip, is
412 illuminated with blue light from a LED, and the voltage across the eye is
413 amplified and recorded. C. Repetitive stimuli given to the fly about a fixed
414 mean light level evoke a contrast response increasing with the peak-peak
415 excursion of the stimulus waveform. D. The response to a series of identical
416 stimuli is analysed by the Fast Fourier Transform, and averaged. This shows a
417 response at the stimulus frequency (1F1) and additional components at
418 multiples of the input, notably twice the input frequency (2F1). Genetic
419 dissection shows that the 1F1 component is mostly generated by the
420 photoreceptors and the 2F1 by the lamina neurons (Afsari *et al.* 2014; Nippe *et*
421 *al.* 2017). E. Plotting the amplitude of the 1F1 and 2F1 components against the
422 stimulus contrast generates a CRF (Contrast Response Function), which
423 differs from fly to fly. F. The averaged maximum CRF is dependent on
424 genotype, with *THG2* (flies expressing *LRRK2-G2019S* in their dopaminergic
425 neurons under the *Tyrosine Hydroxylase*-GAL4, *TH*) and *TH* > *Rab7* both
426 showing a similar mean response to control flies (*TH*/+). However, flies
427 expressing both *G2019S* and *Rab7* in their dopaminergic neurons (*THG2* >
428 *Rab7*) have a larger mean response than any other genotype, indicating
429 synergy. The differences marked X (between the mean *TH*/+ and *TH* > *Rab7*)
430 and Y (between the mean *TH* > *Rab7* and *THG2* > *Rab7*) are used as the X and
431 Y axes of Fig. 2A. Box-plot representing median and interquartile range. Exact

genotypes and sample sizes: *TH/+*, *TH/w*^{1118}, N= 7; *THG2*, *TH::G2019S/ w*^{1118}, N=11; *TH* > *Rab7*, N=11; *THG2* > *Rab7*, N=12.

Fig. 2. **Expression screen highlights *Rab10* with the strongest synergy with *LRRK2-G2019S*, and *Rab3* as the weakest**. Each *Rab* was expressed in dopaminergic neurons (using *TH*-GAL4) by itself (*TH* > *Rab*), or along with *G2019S* (*THG2* > *Rab*) and the visual response measured after 24-36 hours (labelled 1 day) or 7 days in the dark. A. **Rab10 has the strongest synergy with *G2019S*.** Relationship of *Rab* and *G2019S* showing their inverse relationship. Rabs (3, 32, 1) which have a big effect on vision when expressed on their own have little further consequence when *G2019S* is also expressed; but other Rabs (10, 27, 14, 26) which have little visual impact on their own have a strong synergy with *G2019S*. B. **An established role in Parkinson's is the only factor that influences the inverse relationship between *TH > Rab* and *THG2 > Rab***. The LRRK2 ↔ Rab data in Fig. 2A are replotted here to test if it is affected by factors that have been proposed to influence LRRK2 ↔ Rab interactions. (i). Rabs previously linked to Parkinson's (Shi *et al.* 2017) have a stronger Rab ↔ G2019S response than those which do not influence Parkinson's, since a higher proportion of the magenta points lie above the line (Fisher's exact test, P = 0.036). B(ii). Sensitivity is not linked to the phylogenetic grouping of the fly Rabs (Zhang *et al.* 2006) . B(iii). Rabs usually have a serine (Ser) or threonine (Thr) where they could be phosphorylated by LRRK2, though Rab40 has a histidine (His) (Zhang *et al.* 2006). Although a preference for LRRK2 to phosphorylate Rabs with a threonine was suggested by *in vitro* assays (Steger *et al.* 2016), *in vivo* this is not detected. B(iv). Some Rabs are phosphorylated by LRRK2 *in vitro* (Steger *et al.* 2017), but these Rabs are not more sensitive to *G2019S in vivo*. B(v). The proposed main functional role of the Rab (Banworth and Li 2017) does not affect the regression. Total flies: 1119, at least 9 for each data point. Bars represent SE.

Fig. 3. **Standout role of *Rab10* with *G2019S* in neuronal signaling**. The SSVEP response is split into two components, representing the

464 photoreceptors and lamina neurons (inset orange and purple). For each Rab,
465 the increase in lamina neuronal signaling due to *G2019S* is plotted as a
466 function of the photoreceptor signal. The increase in lamina neuron response
467 is highly correlated with the response of the photoreceptors, with one
468 outlying exception, *Rab10* at 1 day. Total flies: 1119, at least 9 for each data
469 point. Bars represent SE.
470
471 Fig. 4. **High sequence homology between *Drosophila* and human Rabs**.
472 Comparison of fly and human Rab10 (A) and Rab3 (B) showing conservation
473 in the GTPase domain and prenylated region. Also shown is the region which
474 is phosphorylated *in vitro* by LRRK2, again highly conserved.
475
476 Fig. 5. **Similar Expression of LRRK2-G2019S and Rab-GFP in dopaminergic**
477 **neurons**. A. Co-expression of a *Rab-GFP* transgene does not affect the levels of
478 *LRRK2-G2019S*. (i) Sample blot, (ii) Quantification of 3 replicates. B. Similar
479 levels of Rab10 and Rab39, and less Rab3 when driven with *LRRK2-G2019S*.
480 (i) Sample blot, (ii) Quantification of 3 replicates. wild-type is *CS/w*$^{-}$, *TH/+* is
481 *TH/empty vector.*
482
483 Fig. 6. **Rab10 and Rab3 are located in different subsets of the dopaminergic**
484 **neurons.** A, B. Rab10 is detected in some of the dopaminergic neurons that
485 control vision (PPL1, Aii, Bii; PPL2 Aiii, Biii). Not all dopaminergic neurons,
486 identified by a cytosolic α-Tyrosine Hydroxylase antibody (α-TH, green), are
487 indicated by *Rab10*-GAL4 expression of a strong nuclear RFP or the mainly
488 nuclear eIf-GFP (magenta). The dopaminergic MC neurons in the visual lobes
489 do not stain well with fluorescent reporters (Nassel and Elekes 1992; Hindle *et*
490 *al.* 2013) and we could not detect *Rab10*-driven fluorescence (MC, Aiv, Biv,
491 marked with grey in E). C, D. **Rab 3 is present in all dopaminergic neurons**.
492 *Rab3*-GAL4 driven nuclear RFP or eIf-GFP (magenta) marks most neurons,
493 including nearly all that are dopaminergic (green). The PPL neurons not
494 marked by *Rab10* expression are included (Dii-iv). E. Summary of the

495 expression pattern of (i) *Rab10* and (ii) *Rab3*. The MC neurons in the optic lobe
496 (Nassel *et al.* 1988) are also called Mi15 neurons (Davis *et al.* 2020). Ai, Bi, Ci
497 and Di: projection of confocal stacks through the whole CNS; Aii, Aiii, Bii,
498 Biii, Dii-iv projections of confocal stacks through the cell groups,
499 approximately marked in the whole CNS image; Aiv and Biv sections from a
500 separate preparation to Ai and Bi. Data representative of at least nine brains
501 (from at least 3 crosses), 3-7 days old. The *Rab3* > *nRFP* flies were raised at 18
502 °C to improve viability. Exact genotypes: +; *RedStinger4 nRFP/+; Rab10 Gal4/+;*
503 or +*; RedStinger4 nRFP/+; Rab3 Gal4/+*; or +; *eIf-4A3-GFP/+; Rab10 Gal4/+;* or +;
504 *eIf-4A3-GFP/+; Rab3 Gal4/+;*
505
506 Fig.7. Differences in neuron survival in dopaminergic clusters when an
507 increased kinase mutation (*G2019S* or *I2020T*) is expressed with *DDC*-GAL4
508 (which expresses in dopaminergic and serotonergic neurons) (ANOVA, 4,45
509 df, $P<0.002$). Data collected from (Liu *et al.* 2008; Ng *et al.* 2009; Xiong *et al.*
510 2012; Angeles *et al.* 2014, 2016; Martin *et al.* 2014; Nucifora *et al.* 2016; Lin *et al.*
511 2016; Sun *et al.* 2016; Basil *et al.* 2017; Marcogliese *et al.* 2017; Yang *et al.* 2018;
512 Lavoy *et al.* 2018; Sim *et al.* 2019; Maksoud *et al.* 2019; Chittoor-Vinod *et al.*
513 2020). Differences in the extent of degeneration within a neuronal cluster may
514 be partially explained by differences in the composition of the fly food
515 (Chittoor-Vinod *et al.* 2020).
516

Acknowledgements. We are grateful for the gifts of flies from Wanli Smith and the Bloomington Drosophila Supply Center. We also thank Olivia Compton and Martin France who helped with pilot studies, the University of York Biology Technology Facility and Flybase. Ian Martin kindly provided unpublished details of dopaminergic cell loss. We are particularly grateful to Parkinson's UK and to their volunteers for support (K-1704, G-1804).

REFERENCES

Afsari, F., K. V. Christensen, G. P. Smith, M. Hentzer, O. M. Nippe *et al.*, 2014 Abnormal visual gain control in a Parkinson's disease model. Hum. Mol. Genet. 23: 4465–4478 doi:10.1093/hmg/ddu159.

Angeles, D. C., P. Ho, L. L. Chua, C. Wang, Y. W. Yap *et al.*, 2014 Thiol-peroxidases ameliorate LRRK2 mutant-induced mitochondrial and dopaminergic neuronal degeneration in Drosophila. Hum. Mol. Genet. doi:10.1093/hmg/ddu026.

Angeles, D. C., P. Ho, B. W. Dymock, K. Lim, Z. Zhou *et al.*, 2016 Antioxidants inhibit neuronal toxicity in Parkinson ' s disease-linked LRRK2. doi:10.1002/acn3.282.

Banworth, M. J., and G. Li, 2017 Consequences of Rab GTPase dysfunction in genetic or acquired human diseases. Small GTPases 1–24 doi:10.1080/21541248.2017.1397833.

Basil, A. H., J. P. L. Sim, G. G. Y. Lim, S. Lin, H. Y. Chan *et al.*, 2017 AF-6 Protects Against Dopaminergic Dysfunction and Mitochondrial Abnormalities in Drosophila Models of Parkinson's Disease. Front. Cell. Neurosci. 11: 241 doi:10.3389/fncel.2017.00241.

Beilina, A., I. N. Rudenko, A. Kaganovich, L. Civiero, H. Chau *et al.*, 2014 Unbiased screen for interactors of leucine-rich repeat kinase 2 supports a common pathway for sporadic and familial Parkinson disease. Proc. Natl. Acad. Sci. 111: 2626–2631 doi:10.1073/pnas.1318306111.

Burbulla, L. F., P. Song, J. R. Mazzulli, E. Zampese, Y. C. Wong *et al.*, 2017 Dopamine oxidation mediates mitochondrial and lysosomal dysfunction in Parkinson's disease. Science (80-.). 357: 1255–1261 doi:10.1126/science.aam9080.

Cajal, S. R., and D. Sanchez, 1915 Contribucion al conocimiento de los centros nerviosos de los insectos. Parte 1. Retina y centros opticos. Trab. Lab Invest. Bio. Univ. Madrid 13: 1–168.

Caviglia, S., M. Brankatschk, E. J. Fischer, S. Eaton, and S. Luschnig, 2016 Staccato/Unc-13-4 controls secretory lysosome-mediated lumen fusion during epithelial tube anastomosis. Nat. Cell Biol. 18: 727–739 doi:10.1038/ncb3374.

Chan, C.-C., S. Scoggin, D. Wang, S. Cherry, T. Dembo *et al.*, 2011 Systematic discovery of Rab GTPases with synaptic functions in Drosophila. Curr.

Biol. 21: 1704–15 doi:10.1016/j.cub.2011.08.058.

Chen, Y., Y. Wang, J. Zhang, Y. Deng, L. Jiang *et al.*, 2012 Rab10 and myosin-Va mediate insulin-stimulated GLUT4 storage vesicle translocation in adipocytes. J. Cell Biol. 198: 545–60 doi:10.1083/jcb.201111091.

Chittoor-Vinod, V. G., S. Villalobos-Cantor, H. Roshak, K. Shea, and I. Martin, 2020 Dietary Amino Acids Impact LRRK2-induced Neurodegeneration in Parkinson's Disease Models. bioRxiv 2020.01.13.905471 doi:10.1101/2020.01.13.905471.

Chua, C. E. L., and B. L. Tang, 2018 Rab 10—a traffic controller in multiple cellular pathways and locations. J. Cell. Physiol. 233: 6483–6494 doi:10.1002/jcp.26503.

Chyb, S., W. Hevers, M. Forte, W. J. Wolfgang, Z. Selinger *et al.*, 1999 Modulation of the light response by cAMP in Drosophila photoreceptors. J. Neurosci. 19: 8799–8807.

Cording, A. C., N. Shiaelis, S. Petridi, C. A. Middleton, L. G. Wilson *et al.*, 2017 Targeted kinase inhibition relieves slowness and tremor in a Drosophila model of LRRK2 Parkinson's. npj Park. Dis. 3: 34 doi:10.1038/s41531-017-0036-y.

Damier, P., E. C. Hirsch, Y. Agid, and A. M. Graybiel, 1999 The substantia nigra of the human brain: II. Patterns of loss of dopamine-containing neurons in Parkinson's disease. Brain 122: 1437–1448 doi:10.1093/brain/122.8.1437.

Davis, F. P., A. Nern, S. Picard, M. B. Reiser, G. M. Rubin *et al.*, 2020 A genetic, genomic, and computational resource for exploring neural circuit function. Elife 9: 1–40 doi:10.1101/385476.

Dodson, M. W., T. Zhang, C. Jiang, S. Chen, and M. Guo, 2012 Roles of the Drosophila LRRK2 homolog in Rab7-dependent lysosomal positioning. Hum. Mol. Genet. 21: 1350–63 doi:10.1093/hmg/ddr573.

Eguchi, T., T. Kuwahara, M. Sakurai, T. Komori, T. Fujimoto *et al.*, 2018 LRRK2 and its substrate Rab GTPases are sequentially targeted onto stressed lysosomes and maintain their homeostasis. Proc. Natl. Acad. Sci. U. S. A. 115: E9115–E9124 doi:10.1073/pnas.1812196115.

Encarnação, M., L. Espada, C. Escrevente, D. Mateus, J. Ramalho *et al.*, 2016 A Rab3a-dependent complex essential for lysosome positioning and plasma membrane repair. J. Cell Biol. 213: 631–40 doi:10.1083/jcb.201511093.

Fan, Y., A. J. M. Howden, A. R. Sarhan, P. Lis, G. Ito *et al.*, 2018 Interrogating Parkinson's disease LRRK2 kinase pathway activity by assessing Rab10 phosphorylation in human neutrophils. Biochem. J. 475: 23–44 doi:10.1042/BCJ20170803.

Fu, Y., J. Zhu, F. Zhang, A. Richman, Z. Zhao *et al.*, 2017 Comprehensive functional analysis of Rab GTPases in Drosophila nephrocytes. Cell Tissue Res. 368: 615–627 doi:10.1007/s00441-017-2575-2.

Fujita, N., W. Huang, T.-H. Lin, J.-F. Groulx, S. Jean *et al.*, 2017 Genetic screen in Drosophila muscle identifies autophagy-mediated T-tubule remodeling and a Rab2 role in autophagy. Elife 6: e23367 doi:10.7554/eLife.23367.

606 Glodowski, D. R., C. C.-H. Chen, H. Schaefer, B. D. Grant, and C. Rongo, 2007
607 RAB-10 regulates glutamate receptor recycling in a cholesterol-
608 dependent endocytosis pathway. Mol. Biol. Cell 18: 4387–96
609 doi:10.1091/mbc.E07-05-0486.
610 Greggio, E., and M. R. Cookson, 2009 Leucine-Rich Repeat Kinase 2 Mutations
611 and Parkinson's Disease: Three Questions. ASN Neuro 1: AN20090007
612 doi:10.1042/AN20090007.
613 Guzman, J. N., J. Sanchez-Padilla, D. Wokosin, J. Kondapalli, E. Ilijic *et al.*,
614 2010 Oxidant stress evoked by pacemaking in dopaminergic neurons is
615 attenuated by DJ-1. Nature 468: 696–700 doi:10.1038/nature09536.
616 Harnois, C., and T. Di Paolo, 1990 Decreased dopamine in the retinas of
617 patients with Parkinson's disease. Invest opthal vis sci 31: 2473.
618 Himmelberg, M. M., R. J. H. West, C. J. H. Elliott, and A. R. Wade, 2017
619 Abnormal visual gain control and excitotoxicity in early-onset
620 Parkinson's disease Drosophila models. J. Neurophysiol. jn.00681.2017
621 doi:10.1152/jn.00681.2017.
622 Hindle, S. J., F. Afsari, M. Stark, C. A. Middleton, G. J. O. Evans *et al.*, 2013
623 Dopaminergic expression of the Parkinsonian gene LRRK2-G2019S leads
624 to non-autonomous visual neurodegeneration, accelerated by increased
625 neural demands for energy. Hum Mol Genet 22: 2129–2140
626 doi:10.1093/hmg/ddt061.
627 Isabella, A. J., and S. Horne-Badovinac, 2016 Rab10-Mediated Secretion
628 Synergizes with Tissue Movement to Build a Polarized Basement
629 Membrane Architecture for Organ Morphogenesis. Dev. Cell 38: 47–60
630 doi:10.1016/j.devcel.2016.06.009.
631 Islam, M. S., H. Nolte, W. Jacob, A. B. Ziegler, S. Pütz *et al.*, 2016 Human
632 R1441C LRRK2 regulates the synaptic vesicle proteome and
633 phosphoproteome in a Drosophila model of Parkinson's disease. Hum.
634 Mol. Genet. 500: 5365–5382 doi:10.1093/hmg/ddw352.
635 Jaldin-Fincati, J. R., M. Pavarotti, S. Frendo-Cumbo, P. J. Bilan, and A. Klip,
636 2017 Update on GLUT4 Vesicle Traffic: A Cornerstone of Insulin Action.
637 Trends Endocrinol. Metab. 28: 597–611 doi:10.1016/J.TEM.2017.05.002.
638 Jeong, G. R., E.-H. Jang, J. R. Bae, S. Jun, H. C. Kang *et al.*, 2018 Dysregulated
639 phosphorylation of Rab GTPases by LRRK2 induces neurodegeneration.
640 Mol. Neurodegener. 13: 8 doi:10.1186/s13024-018-0240-1.
641 Kelly, K., S. Wang, R. Boddu, Z. Liu, O. Moukha-Chafiq *et al.*, 2018 The
642 G2019S mutation in LRRK2 imparts resiliency to kinase inhibition. Exp.
643 Neurol. 309: 1–13 doi:10.1016/J.EXPNEUROL.2018.07.012.
644 Kiral, F. R., F. E. Kohrs, E. J. Jin, and P. R. Hiesinger, 2018 Rab GTPases and
645 Membrane Trafficking in Neurodegeneration. Curr. Biol. 28: R471–R486
646 doi:10.1016/j.cub.2018.02.010.
647 Larance, M., G. Ramm, J. Stöckli, E. M. van Dam, S. Winata *et al.*, 2005
648 Characterization of the Role of the Rab GTPase-activating Protein AS160
649 in Insulin-regulated GLUT4 Trafficking. J. Biol. Chem. 280: 37803–37813
650 doi:10.1074/jbc.M503897200.
651 Lavoy, S., V. G. Chittoor-Vinod, C. Y. Chow, and I. Martin, 2018 Genetic

652 Modifiers of Neurodegeneration in a Drosophila Model of Parkinson's
653 Disease. Genetics 209: 1345–1356 doi:10.1534/genetics.118.301119.
654 Lin, C.-H., H.-I. Lin, M.-L. Chen, T.-T. Lai, L.-P. Cao *et al.*, 2016 Lovastatin
655 protects neurite degeneration in LRRK2-G2019S parkinsonism through
656 activating the Akt/Nrf pathway and inhibiting GSK3β activity. Hum.
657 Mol. Genet. 25: 1965–1978 doi:10.1093/hmg/ddw068.
658 Liu, Z., N. Bryant, R. Kumaran, A. Beilina, A. Abeliovich *et al.*, 2018 LRRK2
659 phosphorylates membrane-bound Rabs and is activated by GTP-bound
660 Rab7L1 to promote recruitment to the trans-Golgi network. Hum. Mol.
661 Genet. 27: 385–395 doi:10.1093/hmg/ddx410.
662 Liu, Z., X. Wang, Y. Yu, X. Li, T. Wang *et al.*, 2008 A Drosophila model for
663 LRRK2-linked parkinsonism. Proc. Natl. Acad. Sci. U. S. A. 105: 2693–8
664 doi:10.1073/pnas.0708452105.
665 MacLeod, D. A., H. Rhinn, T. Kuwahara, A. Zolin, G. Di Paolo *et al.*, 2013
666 RAB7L1 interacts with LRRK2 to modify intraneuronal protein sorting
667 and Parkinson's disease risk. Neuron 77: 425–39
668 doi:10.1016/j.neuron.2012.11.033.
669 Maksoud, E., E. H. Liao, and A. P. Haghighi, 2019 A Neuron-Glial Trans-
670 Signaling Cascade Mediates LRRK2-Induced Neurodegeneration. Cell
671 Rep. 26: 1774-1786.e4 doi:10.1016/j.celrep.2019.01.077.
672 Marcogliese, P. C., S. Abuaish, G. Kabbach, E. Abdel-Messih, S. Seang *et al.*,
673 2017 LRRK2(I2020T) functional genetic interactors that modify eye
674 degeneration and dopaminergic cell loss in Drosophila. Hum. Mol.
675 Genet. 26: 1247–1257 doi:10.1093/hmg/ddx030.
676 Martin, I., J. W. Kim, B. D. Lee, H. C. Kang, J.-C. Xu *et al.*, 2014 Ribosomal
677 Protein s15 Phosphorylation Mediates LRRK2 Neurodegeneration in
678 Parkinson's Disease. Cell 157: 472–485 doi:10.1016/j.cell.2014.01.064.
679 Nassel, D. R., and K. Elekes, 1992 Aminergic neurons in the brain of blowflies
680 and Drosophila: dopamine- and tyrosine hydroxylase-immunoreactive
681 neurons and their relationship with putative histaminergic neurons. Cell
682 Tissue Res. 267: 147–167 doi:10.1007/bf00318701.
683 Nassel, D. R., K. Elekes, K. U. Johansson, and D. R. Nässel, 1988 Dopamine-
684 immunoreactive neurons in the blowfly visual system: light and electron
685 microscopic immunocytochemistry. J. Chem. Neuroanat. 1: 311–325.
686 Ng, C.-H. H., S. Z. S. Mok, C. Koh, X. Ouyang, M. L. Fivaz *et al.*, 2009 Parkin
687 Protects against LRRK2 G2019S Mutant-Induced Dopaminergic
688 Neurodegeneration in Drosophila. J Neurosci. 29: 11257–11262
689 doi:10.1523/JNEUROSCI.2375-09.2009.
690 Nippe, O. M., A. R. Wade, C. J. H. Elliott, and S. Chawla, 2017 Circadian
691 Rhythms in Visual Responsiveness in the Behaviorally Arrhythmic
692 Drosophila Clock Mutant Clk Jrk. J. Biol. Rhythms 32: 583–592
693 doi:10.1177/0748730417735397.
694 Nucifora, F. C., L. G. Nucifora, C. H. Ng, N. Arbez, Y. Guo *et al.*, 2016
695 Ubiqutination via K27 and K29 chains signals aggregation and neuronal
696 protection of LRRK2 by WSB1. Nat. Commun. 7: 1–11
697 doi:10.1038/ncomms11792.

698 Ostrowski, M., N. B. Carmo, S. Krumeich, I. Fanget, G. Raposo *et al.*, 2010
699 Rab27a and Rab27b control different steps of the exosome secretion
700 pathway. Nat. Cell Biol. 12: 19–30; sup pp 1-13 doi:10.1038/ncb2000.
701 Pacelli, C., N. Giguère, M.-J. Bourque, M. Lévesque, R. S. Slack *et al.*, 2015
702 Elevated Mitochondrial Bioenergetics and Axonal Arborization Size Are
703 Key Contributors to the Vulnerability of Dopamine Neurons. Curr. Biol.
704 25: 2349–2360 doi:10.1016/j.cub.2015.07.050.
705 Purlyte, E., H. S. Dhekne, A. R. Sarhan, R. Gomez, P. Lis *et al.*, 2018 Rab29
706 activation of the Parkinson's disease-associated LRRK2 kinase. EMBO J.
707 37: 1–18 doi:10.15252/embj.201798099.
708 Sanes, J. R., and S. L. Zipursky, 2010 Design principles of insect and vertebrate
709 visual systems. Neuron 66: 15–36 doi:10.1016/j.neuron.2010.01.018.
710 Shi, M., C.-H. Shi, and Y. Xu, 2017 Rab GTPases: The Key Players in the
711 Molecular Pathway of Parkinson's Disease. Front. Cell. Neurosci. 11: 81
712 doi:10.3389/fncel.2017.00081.
713 Shin, N., H. Jeong, J. Kwon, H. Y. Heo, J. J. Kwon *et al.*, 2008 LRRK2 regulates
714 synaptic vesicle endocytosis. Exp. Cell Res. 314: 2055–65
715 doi:10.1016/j.yexcr.2008.02.015.
716 Sim, J. P. L., W. Ziyin, A. H. Basil, S. Lin, Z. Chen *et al.*, 2019 Identification of
717 PP2A and S6 Kinase as Modifiers of Leucine-Rich Repeat Kinase-Induced
718 Neurotoxicity. NeuroMolecular Med. doi:10.1007/s12017-019-08577-z.
719 Steger, M., F. Diez, H. S. Dhekne, P. Lis, R. S. Nirujogi *et al.*, 2017 Systematic
720 proteomic analysis of LRRK2-mediated Rab GTPase phosphorylation
721 establishes a connection to ciliogenesis. Elife 6: e31012
722 doi:10.7554/eLife.31012.
723 Steger, M., F. Tonelli, G. Ito, P. Davies, M. Trost *et al.*, 2016
724 Phosphoproteomics reveals that Parkinson's disease kinase LRRK2
725 regulates a subset of Rab GTPases. Elife 5: doi:10.7554/eLife.12813.
726 Steinkellner, T., V. Zell, Z. J. Farino, M. S. Sonders, M. Villeneuve *et al.*, 2018
727 Role for VGLUT2 in selective vulnerability of midbrain dopamine
728 neurons. J. Clin. Invest. 128: 774–788 doi:10.1172/JCI95795.
729 Subramaniam, M., D. Althof, S. Gispert, J. Schwenk, G. Auburger *et al.*, 2014
730 Mutant -Synuclein Enhances Firing Frequencies in Dopamine Substantia
731 Nigra Neurons by Oxidative Impairment of A-Type Potassium Channels.
732 J. Neurosci. 34: 13586–13599 doi:10.1523/JNEUROSCI.5069-13.2014.
733 Sun, X., D. Ran, X. Zhao, Y. Huang, S. Long *et al.*, 2016 Melatonin attenuates
734 hLRRK2-induced sleep disturbances and synaptic dysfunction in a
735 Drosophila model of Parkinson's disease. Mol. Med. Rep. 13: 3936–3944
736 doi:10.3892/mmr.2016.4991.
737 Thirstrup, K., J. C. Dächsel, F. S. Oppermann, D. S. Williamson, G. P. Smith *et*
738 *al.*, 2017 Selective LRRK2 kinase inhibition reduces phosphorylation of
739 endogenous Rab10 and Rab12 in human peripheral mononuclear blood
740 cells. Sci. Rep. 7: 10300 doi:10.1038/s41598-017-10501-z.
741 Tomkins, J. E., S. Dihanich, A. Beilina, R. Ferrari, N. Ilacqua *et al.*, 2018
742 Comparative Protein Interaction Network Analysis Identifies Shared and
743 Distinct Functions for the Human ROCO Proteins. Proteomics 18:

744 e1700444 doi:10.1002/pmic.201700444.
745 Vieira, O. V., 2018 Rab3a and Rab10 are regulators of lysosome exocytosis and
746 plasma membrane repair. Small GTPases 9: 349–351
747 doi:10.1080/21541248.2016.1235004.
748 Wang, C., Z. Liu, and X. Huang, 2012 Rab32 is important for autophagy and
749 lipid storage in Drosophila. PLoS One 7: e32086
750 doi:10.1371/journal.pone.0032086.
751 Wauters, F., T. Cornelissen, D. Imberechts, S. Martin, B. Koentjoro *et al.*, 2019
752 LRRK2 mutations impair depolarization-induced mitophagy through
753 inhibition of mitochondrial accumulation of RAB10. Autophagy 16: 203–
754 222 doi:10.1080/15548627.2019.1603548.
755 West, R. J. H., R. Furmston, C. A. C. Williams, and C. J. H. Elliott, 2015a
756 Neurophysiology of Drosophila models of Parkinson's disease.
757 Parkinsons. Dis. 2015: 381281
758 doi:http://dx.doi.org/10.1155/2015/381281.
759 West, R. J. H., Y. Lu, B. Marie, F.-B. Gao, and S. T. Sweeney, 2015b Rab8,
760 POSH, and TAK1 regulate synaptic growth in a Drosophila model of
761 frontotemporal dementia. J. Cell Biol. 208: 931–47
762 doi:10.1083/jcb.201404066.
763 White, J. A., E. Anderson, K. Zimmerman, K. H. Zheng, R. Rouhani *et al.*, 2015
764 Huntingtin differentially regulates the axonal transport of a sub-set of
765 Rab-containing vesicles in vivo. Hum. Mol. Genet. 24: 7182–95
766 doi:10.1093/hmg/ddv415.
767 Wilson, G. R., J. C. H. Sim, C. McLean, M. Giannandrea, C. A. Galea *et al.*,
768 2014 Mutations in RAB39B cause X-linked intellectual disability and
769 early-onset Parkinson disease with α-synuclein pathology. Am. J. Hum.
770 Genet. 95: 729–35 doi:10.1016/j.ajhg.2014.10.015.
771 Xiong, Y., C. Yuan, R. Chen, T. M. Dawson, and V. L. Dawson, 2012 ArfGAP1
772 is a GTPase activating protein for LRRK2: reciprocal regulation of
773 ArfGAP1 by LRRK2. J. Neurosci. 32: 3877–86
774 doi:10.1523/JNEUROSCI.4566-11.2012.
775 Yang, D., J. M. Thomas, T. Li, Y. Lee, Z. Liu *et al.*, 2018 The Drosophila hep
776 pathway mediates Lrrk2-induced neurodegeneration. Biochem. Cell Biol.
777 96: 441–449 doi:10.1139/bcb-2017-0262.
778 Zhang, J., K. L. Schulze, P. R. Hiesinger, K. Suyama, S. Wang *et al.*, 2006
779 Thirty-One Flavors of Drosophila Rab Proteins. Genetics 176: 1307–1322
780 doi:10.1534/genetics.106.066761.
781
782

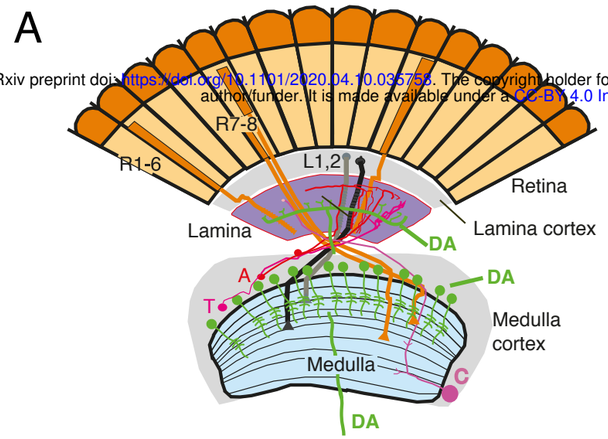

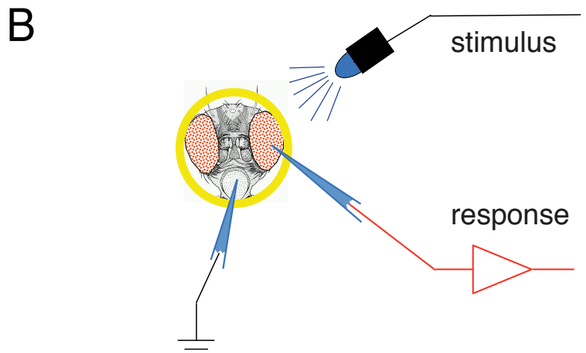

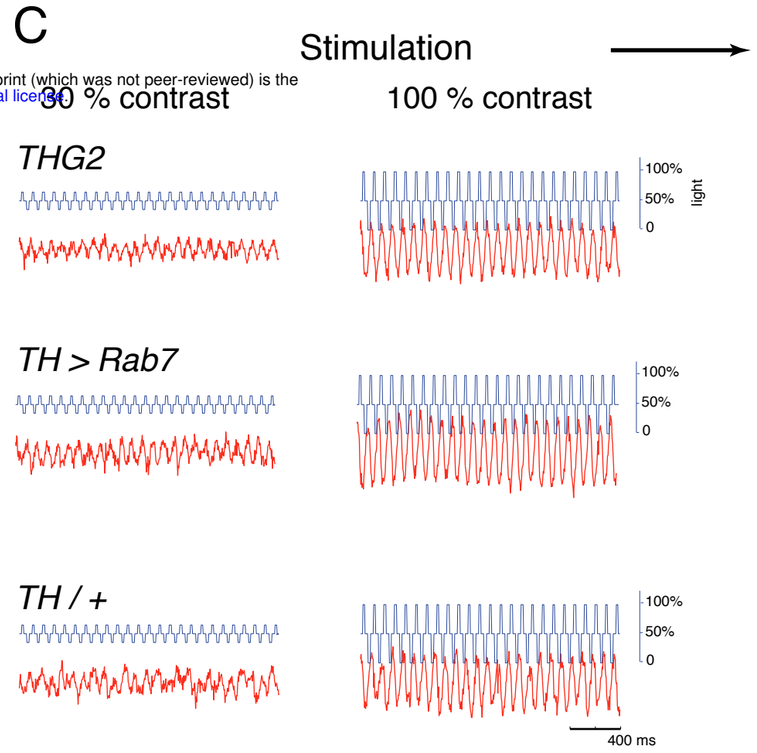

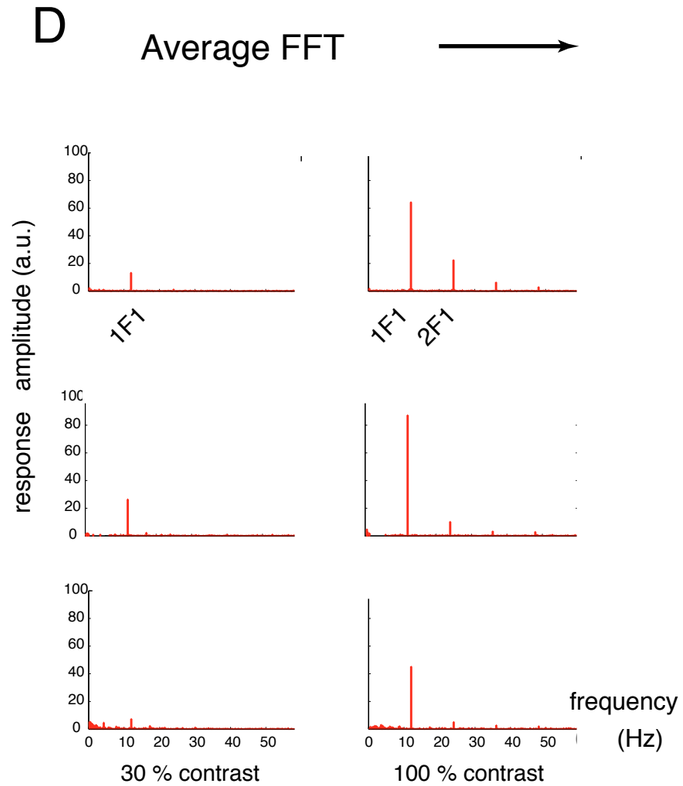

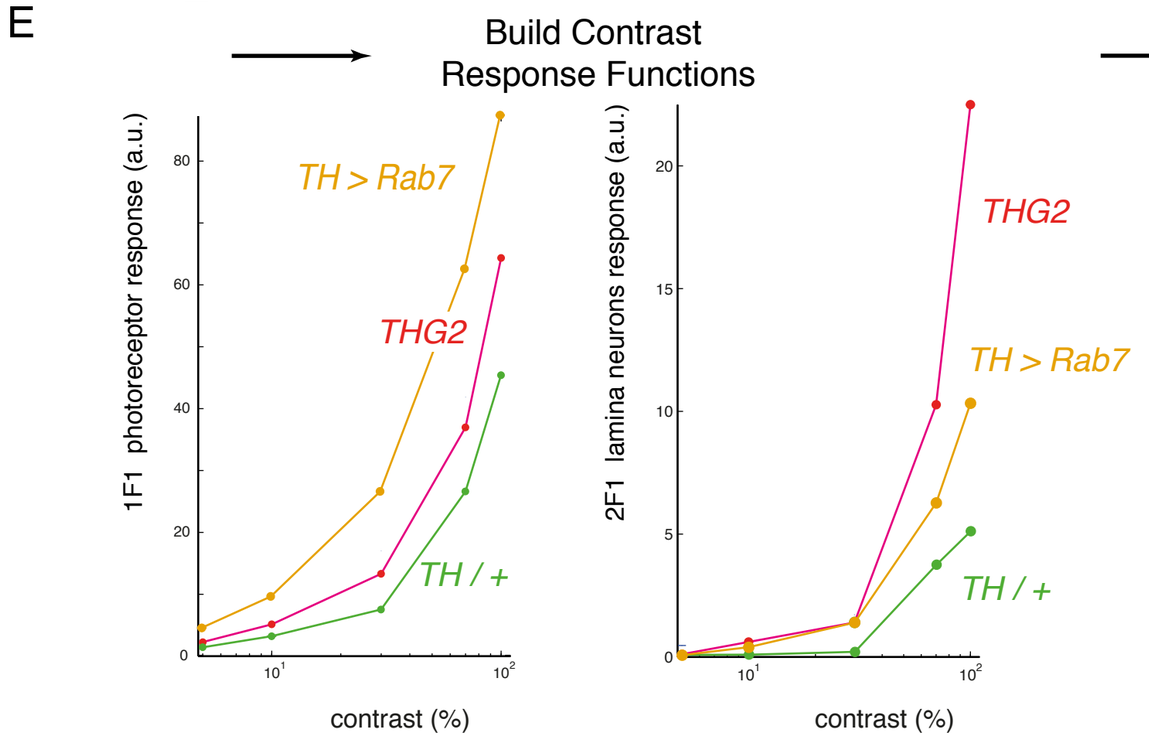

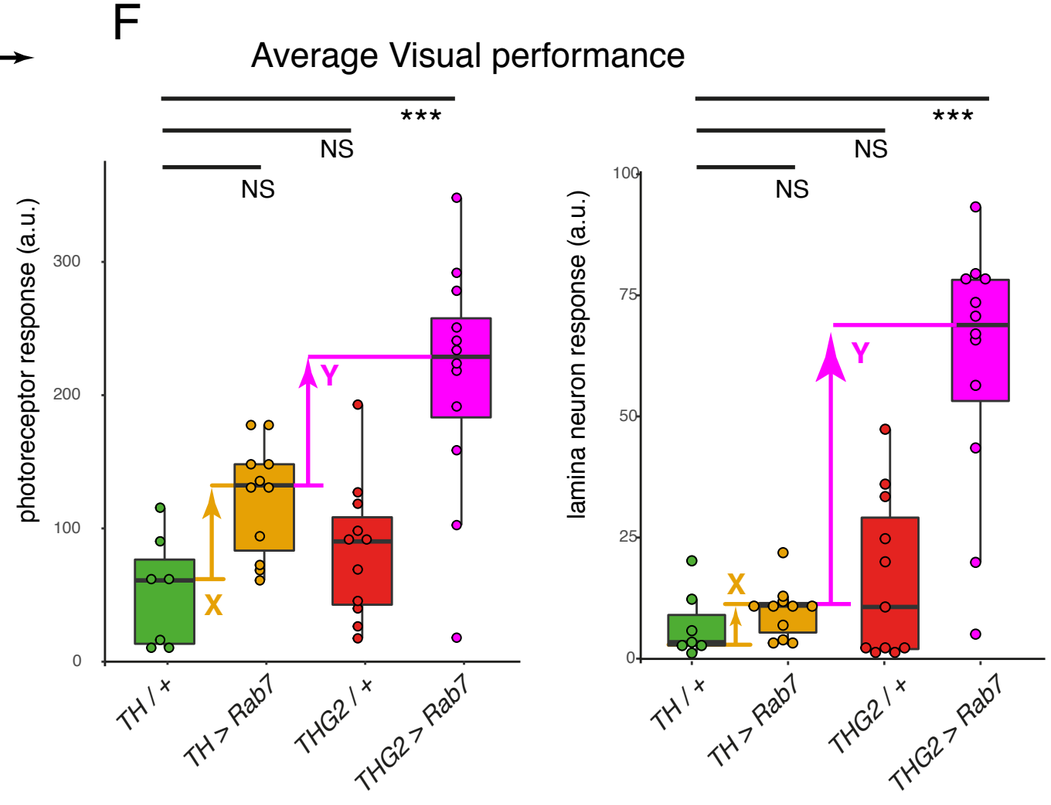

A

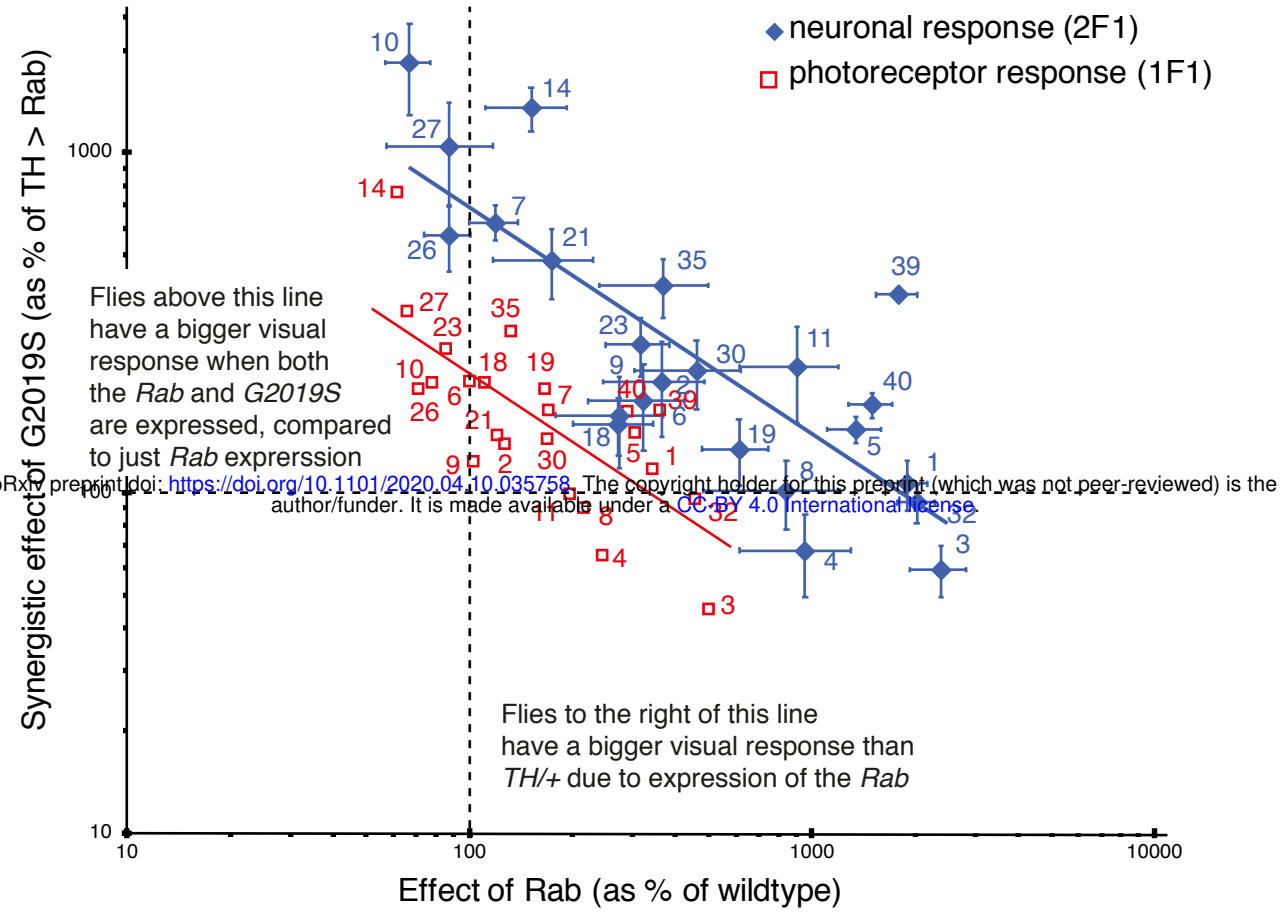

B

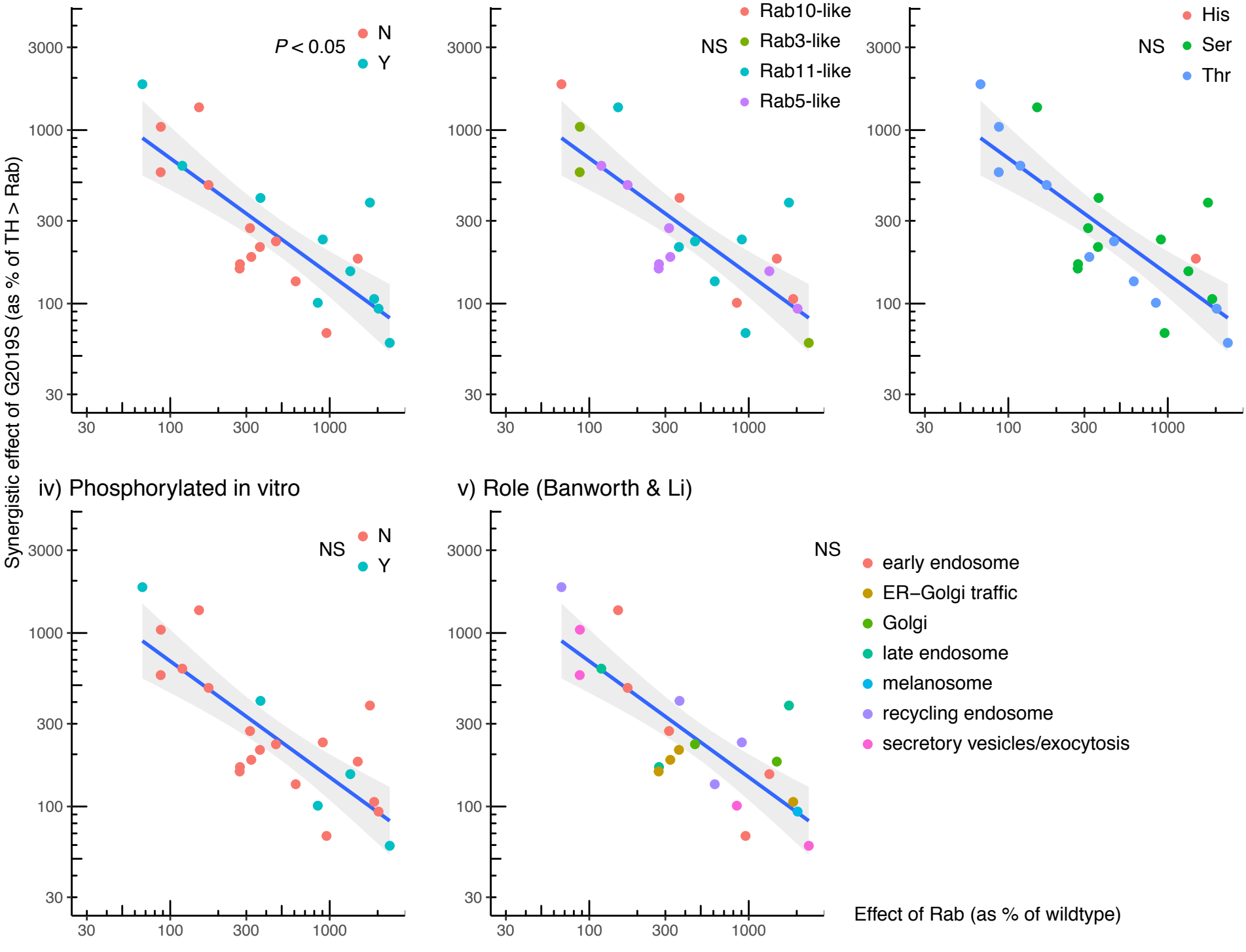

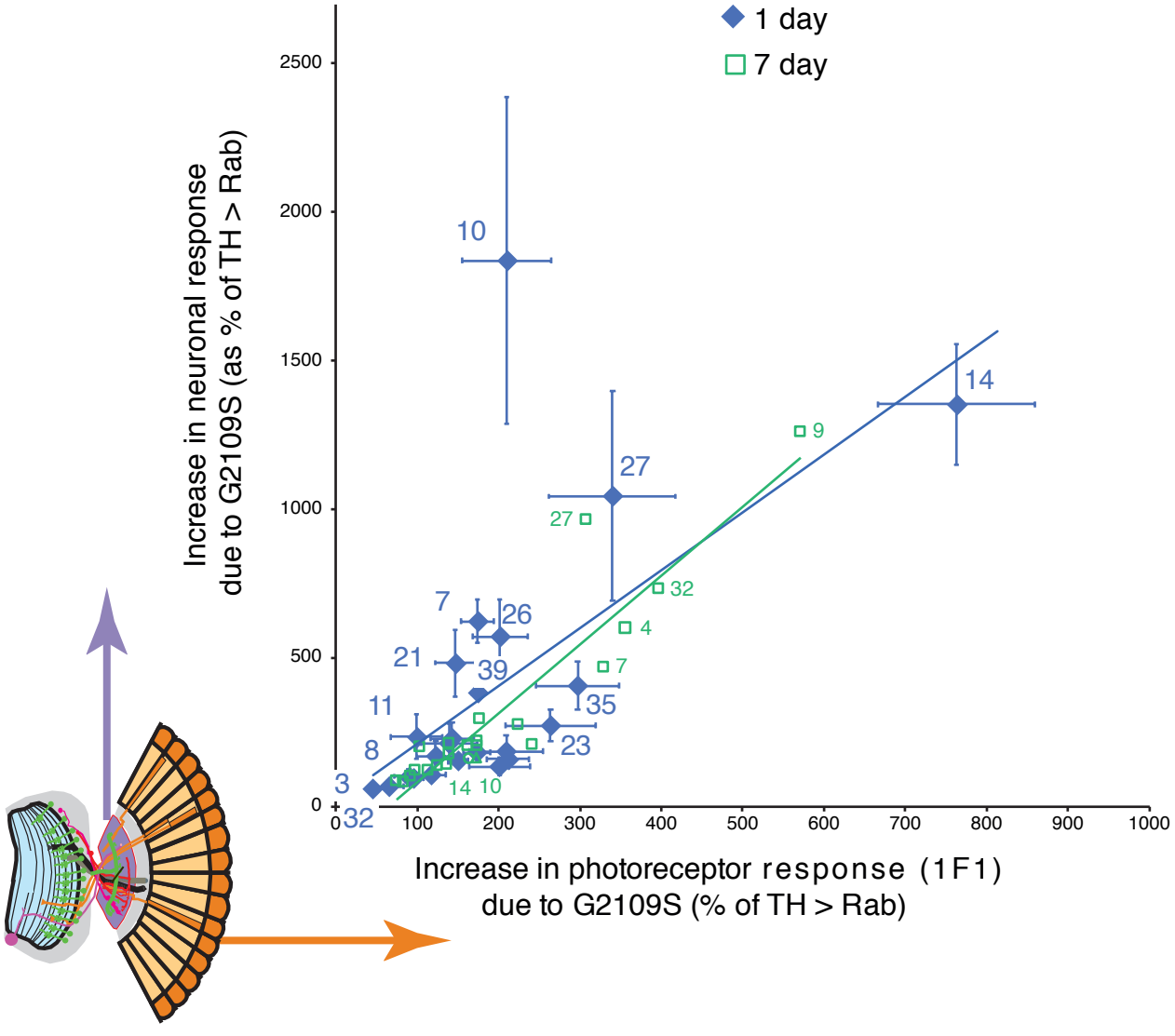
1 day
7 day
Increase in neuronal response
due to G2109S (as % of TH > Rab)
2500
2000
1500
1000
500
0
0
100
200
300
400
500
600
700
800
900
1000
Increase in photoreceptor response (1F1)
due to G2109S (% of TH > Rab)
10
14
27
27
9
32
4
7
26
7
21
39
35
11
23
8
3
14
10
32

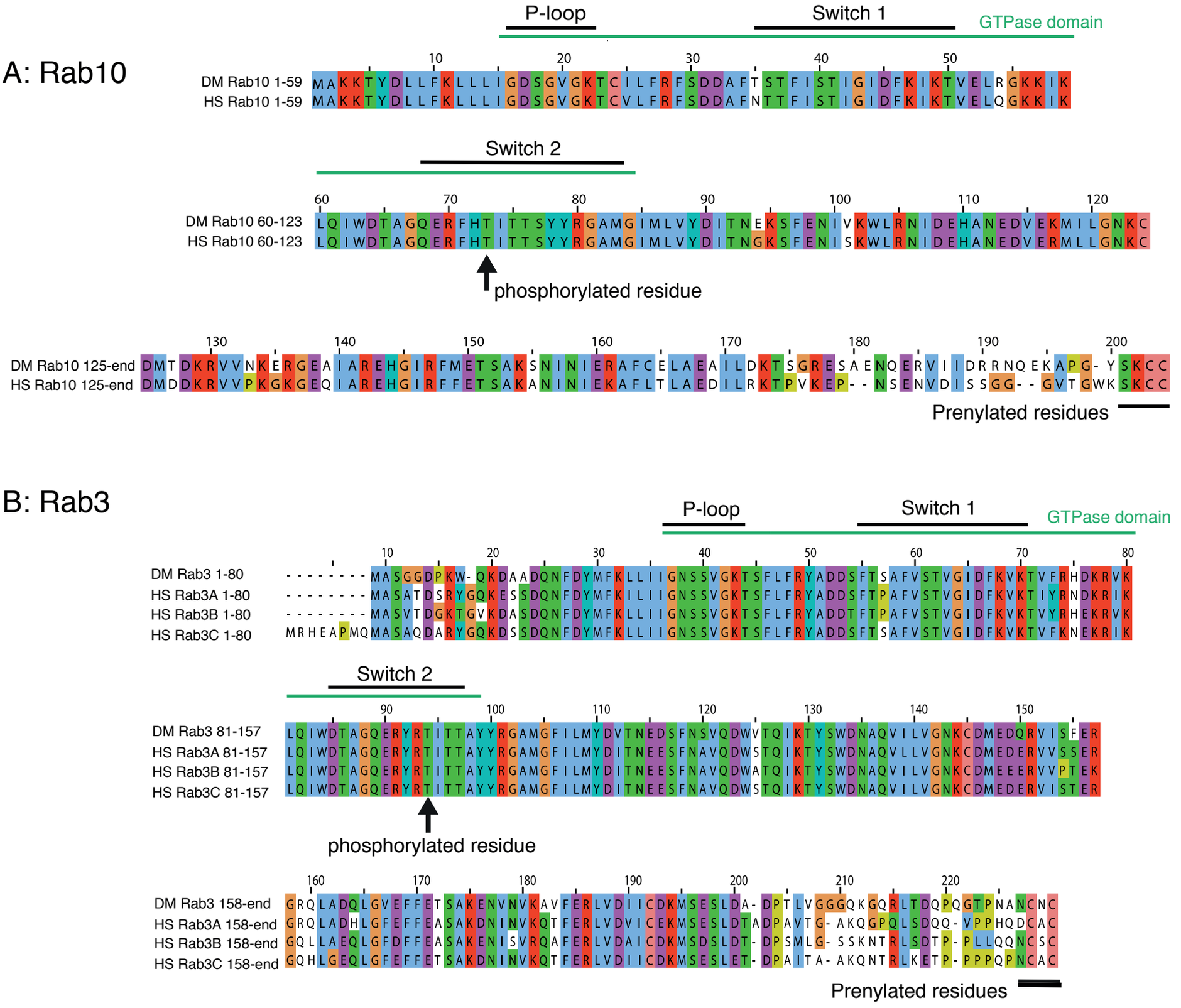
A: Rab10
P-loop
Switch 1
GTPase domain
DM Rab10 1-59
HS Rab10 1-59
Switch 2
DM Rab10 60-123
HS Rab10 60-123
phosphorylated residue
DM Rab10 125-end
HS Rab10 125-end
Prenylated residues
B: Rab3
P-loop
Switch 1
GTPase domain
DM Rab3 1-80
HS Rab3A 1-80
HS Rab3B 1-80
HS Rab3C 1-80
Switch 2
DM Rab3 81-157
HS Rab3A 81-157
HS Rab3B 81-157
HS Rab3C 81-157
phosphorylated residue
DM Rab3 158-end
HS Rab3A 158-end
HS Rab3B 158-end
HS Rab3C 158-end
Prenylated residues

A i

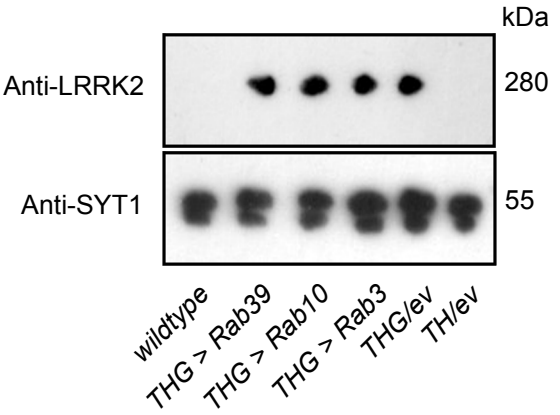

ii

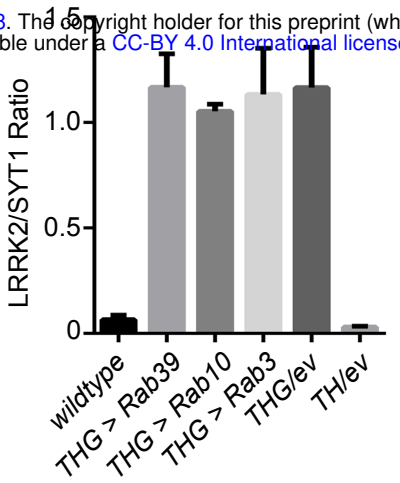

B i

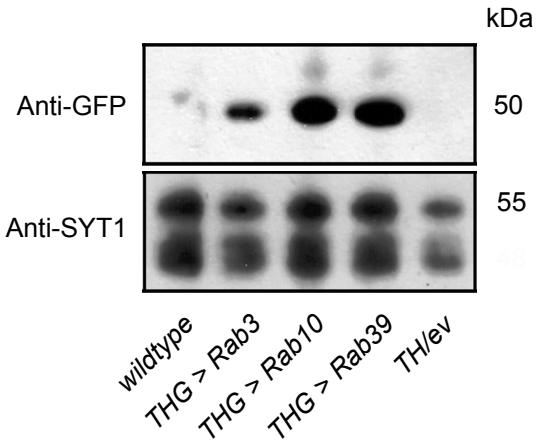

ii

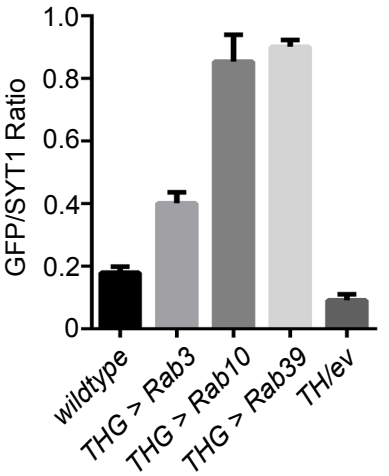

A **Rab10 > nRFP; α-TH**

i whole CNS

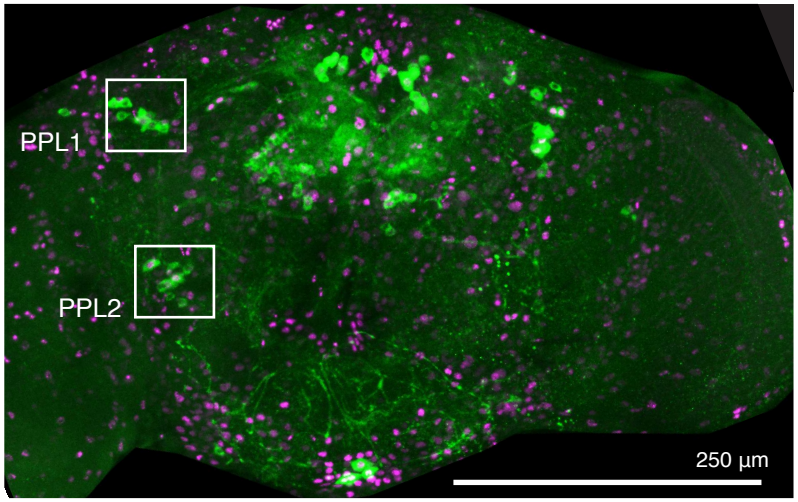

ii PPL1

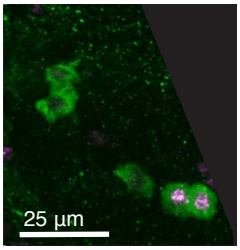

iii PPL2

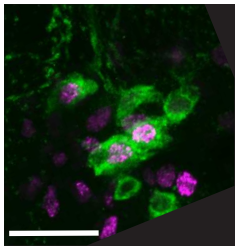

iv MC

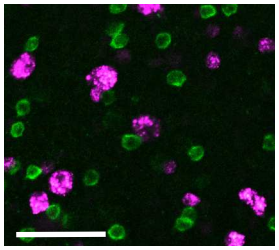

B **Rab10 > elf-GFP; α-TH**

i whole CNS

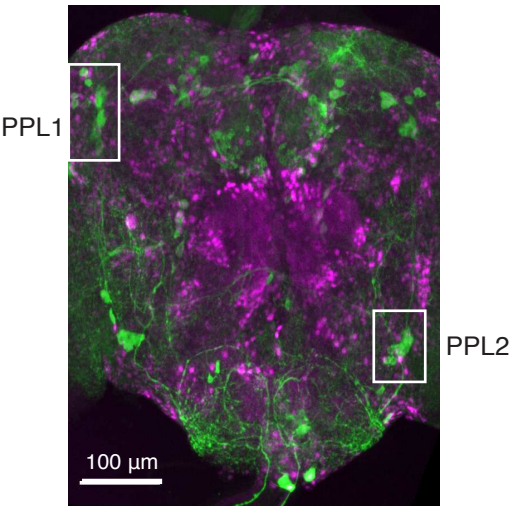

ii PPL1

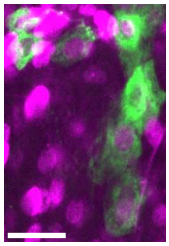

iii PPL2

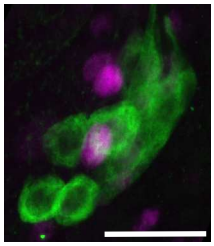

iv MC

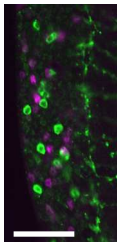

C **Rab3 > nRFP; α-TH**

whole CNS

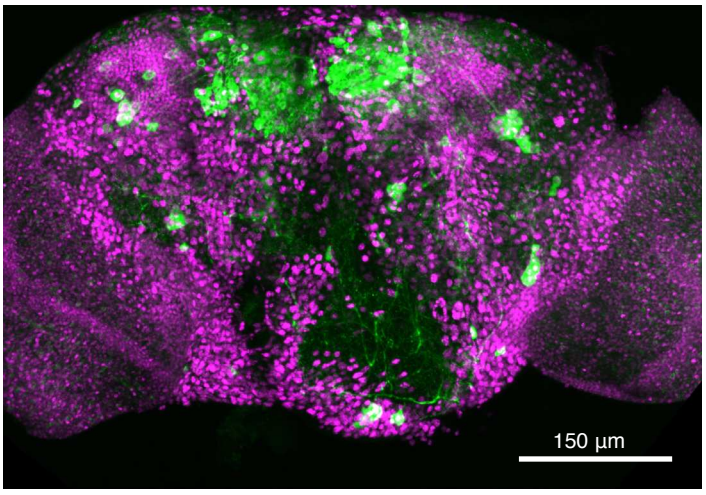

D **Rab3 > elf-GFP; α-TH**

i whole CNS

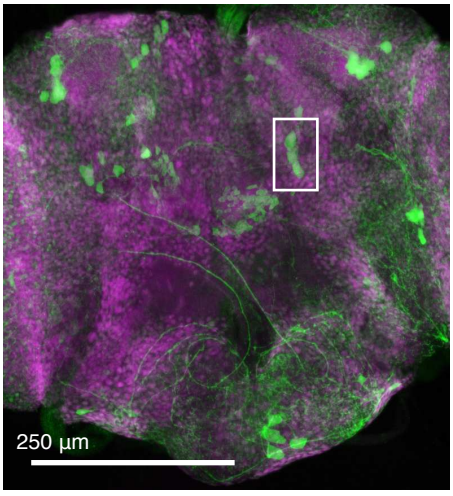

ii PPL1

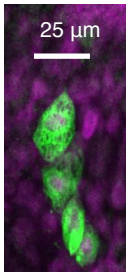

iii elf-GFP

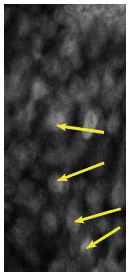

iv α-TH

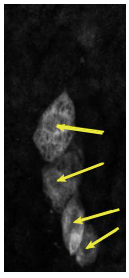

E **Summary**

i Rab10

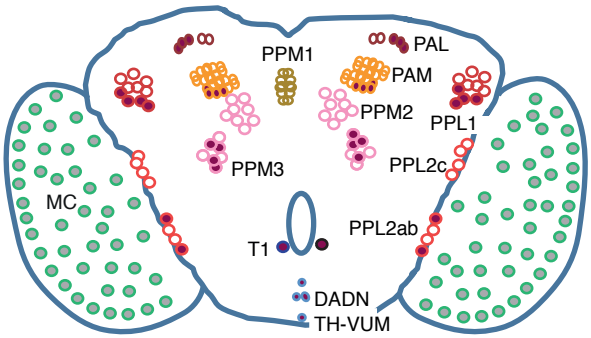

ii Rab3

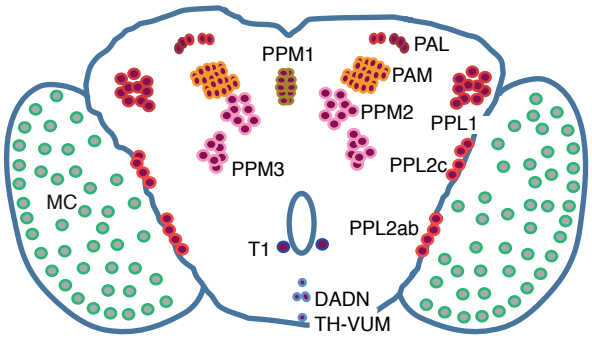

● detected ○ undetectable ◎ undetermined

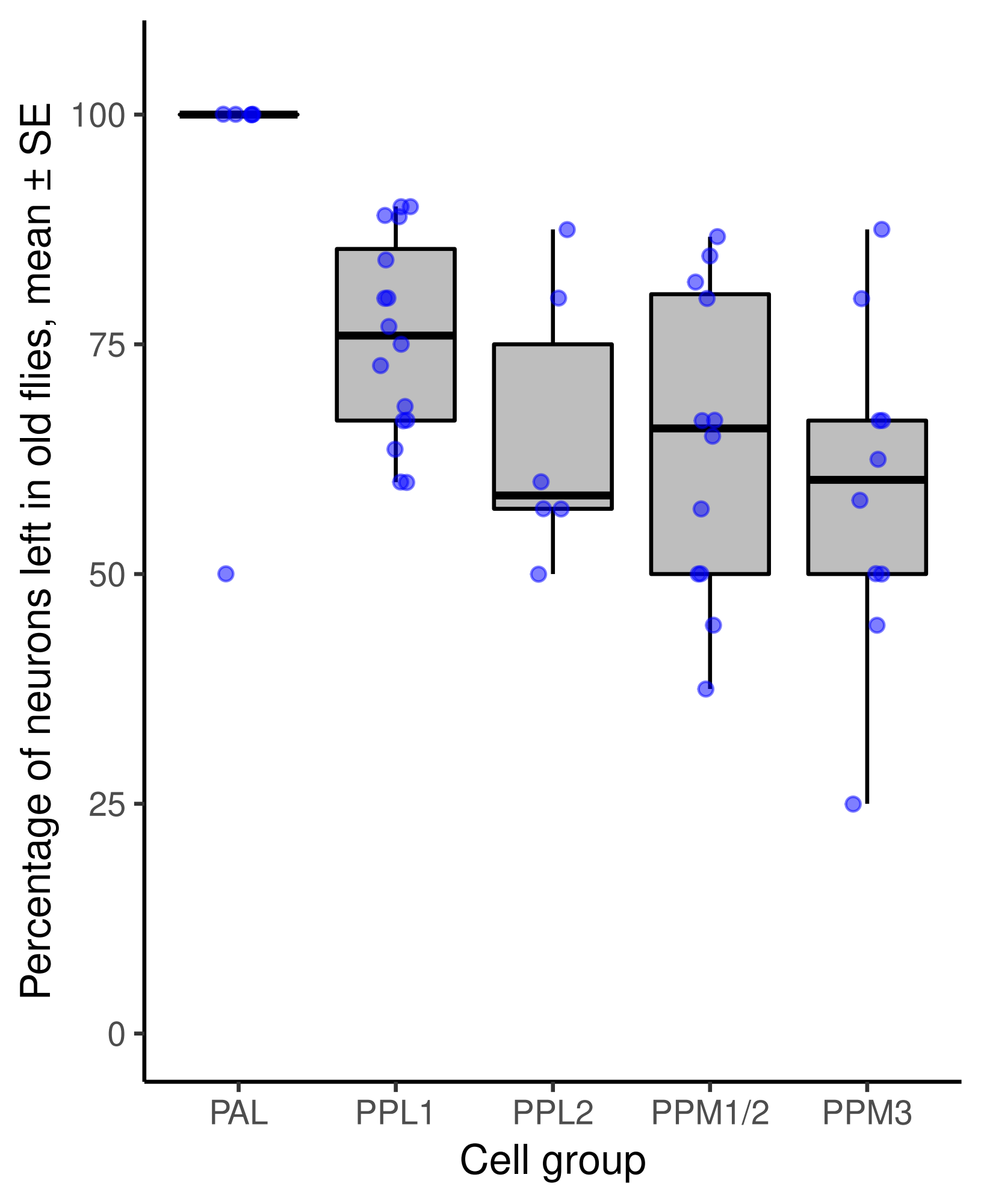
Percentage of neurons left in old flies, mean ± SE
100
75
50
25
0
PAL
PPL1
PPL2
PPM1/2
PPM3
Cell group